Appl. Magn. Reson. 16, 185–205 (1999)

Applied Magnetic Resonance

The Bruker High-Frequency-EPR System

D. Schmalbein, G. G. Maresch*, A. Kamlowski, and P. Höfer

Bruker Analytik GmbH, Rheinstetten, Germany

Received November 12, 1998; revised March 2, 1999

Abstract. The design and performance of the first commercial 94 GHz continuous-wave (CW-)/Fourier transform (FT-) EPR and ENDOR spectrometer are described. The spectrometer design is based on a heterodyne microwave bridge using an X-band intermediate frequency (IF), a hybrid magnet system, a variable-temperature, top-loading TeraFlex probehead with a TE_{011} cavity as well as the ELEXSYS-line digital electronics and the Xepr software package. The W-band bridge can be driven by a CW- or pulse-IF unit and delivers a microwave power of 5 mW at 94 GHz. In pulse mode the power is sufficient for a $\pi/2$ pulse of 100 ns at a resonator Q-value of 3000. The magnet system consists of a 6 T split-coil superconducting magnet and a water-cooled room-temperature coil. The main coil can be swept over the full range from 0 to 6 T. The room-temperature coil has a 800 G sweep range around the persistent field of the main magnet. The ENDOR probe features a tuned circuit for ^1H nuclei allowing an RF π-pulse of 8 μs with a 200 W amplifier. A broad-band setup is used for other nuclei. The E680 FT-EPR system utilizes the PatternJet pulse programmer and the SpecJet high-speed transient signal averager. The concerted action of these two devices results in a pulse EPR sensitivity equal or higher than in CW-EPR. Selected examples indicating the performance of the 94 GHz CW/FT-EPR and ENDOR systems are shown.

1 Introduction

X-band spectrometers have been the standard in electron paramagnetic resonance (EPR) and will remain so. They employ resonance frequencies between 9 and 10 GHz and require magnetic fields typically less than one Tesla (10^4 G). CW and pulsed X-band spectrometers are widely used for applications in physics, chemistry, and biology [1, 2].

The choice of other operating frequencies is mainly governed by the specific properties of the sample, the spin Hamiltonian parameters as well as the aim of the study. In vivo EPR imaging of, for example, small animals, requires frequencies down to a few hundred MHz in order to achieve the required resonator size and to enhance the RF (radio frequency) penetration depth. On the

---

* Present address: National High Magnetic Field Laboratory, Florida State University, 1800 E. Paul Dirac Drive, Tallahassee, Florida 32310, USA

other hand, high-frequency EPR has emerged in recent years as the method of choice to achieve a higher *g*-factor resolution, to gain in sensitivity for limited sample quantities, to extend the range of accessible zero-field splittings and to change the sensitive frequency window for motional effects.

The field of high-frequency EPR was started by Lebedev and co-workers in the 1970s. Since then, in quite a number of labs high-frequency spectrometers have been constructed. Their operation frequency ranges from about 90 GHz, referred to as W-band, to the quasioptical domain of up to 600 GHz with infrared lasers as radiation source. In addition, these home-built spectrometers are capable of either CW-EPR and/or pulsed EPR as well as electron nuclear double resonance (ENDOR). Since 1996, Bruker offers the first commercially available high-frequency spectrometers working at 94 GHz. These W-band systems can operate in either CW or pulsed mode. In the following, some key contributions to high-frequency EPR are mentioned. Note that this listing is by no means complete.

One of the pioneering high-frequency works of Lebedev et al. dealt with a systematic study of nitroxide spin labels [3]. The molecular motions of nitroxide radicals dissolved in a mixture of glycerol and water or in toluene were deduced from EPR spectra taken at 125 GHz [4]. At a resonance frequency of 140 GHz, the structures of phenoxyl radicals including Coppinger's radicals were investigated [5]. For accurate determination of the *g*-tensor components, the EPR signal from Mn^{2+} in MgO powder was used for calibration proposes. The absolute error in the obtained *g*-values was given as $\Delta g = \pm 0.00005$, which corresponds to a relative error of $2.5 \cdot 10^{-5}$. High-frequency EPR imaging at 140 GHz was performed on a TCNQ (7,7,8,8-tetracyanoquinodimethane) crystal, on PCPM (perchlorotriphenylmethyl) radicals in toluene, as well as on TEMPOL (4-hydroxy-2,2,6,6-tetramethylpiperidine-1-oxyl) in frozen water [6]. Pulsed EPR at this frequency was done on TCNQ and irradiated quartz [7].

Another pioneering work was initiated by Möbius et al. with the construction of a 94 GHz EPR spectrometer using a Fabry-Perot resonator [8]. The sensitivity was determined to 10^9 spins per Gauss on a 100 μM solution of TANOL in toluene. The smallest linewidth detected with this spectrometer was 50 mG [9]. Proton ENDOR at 97 GHz microwave frequency in the Fabry-Perot resonator was performed on γ-irradiated α-aminoisobutyric acid at 100 K [10]. W-band CW-EPR single-crystal studies [11] and transient nutation and electron spin echo (ESE) experiments [12] on radical states in the photosynthetic reaction centers of *Rhodobacter sphaeroides* led to the unequivocal assignment of the *g*-tensor principal axes to the molecular structure of the primary donor, P_{865}^{+}. From the characteristic polarization pattern of the transient W-band spectrum it was argued that the spatial orientation of P_{865} and the acceptor quinone, Q_A, does not change much due to light-induced charge-separation.

250 GHz EPR spectra from polycrystalline DPPH and TEMPONE (4-oxo-tetramethylpiperidine-1-oxyl) dissolved in *n*-decane and mineral oil confirm the significant resolution improvement of high-frequency EPR [13]. With high precision the models of rotational diffusion have been evaluated with respect to nitroxides in the slow-motional regime [14].

A pulsed EPR spectrometer operating at 95 GHz was constructed by Schmidt and co-workers [15]. Its performance has been assessed and compared to an X-band pulse spectrometer. From the ESE powder spectrum of a FARCS (fluoranthenyl radical cation salt) sample, the principal g-tensor components of $g_{\parallel} = 2.00258$ and $g_{\perp} = 2.00224$ of the FARCS could nicely be resolved. The minimum number of detectable spins in a single-shot experiment was determined to $5 \cdot 10^{11}$ (for a bandwidth of 20 MHz) using a sample containing $3 \cdot 10^{13}$ biphenyl radicals in boric acid glass. Pulsed EPR and pulsed ENDOR experiments at 95 GHz were conducted to study shallow electron centers in AgCl [16]. This example for nuclei with small gyromagnetic ratios shows that the signals from the two silver isotopes, ^{107}Ag and ^{109}Ag, and the two chlorine isotopes, ^{35}Cl and ^{37}Cl, could clearly be separated by high-frequency ENDOR. ODMR (optically detected magnetic resonance) employing 95 GHz microwave frequencies was performed to unravel dynamical properties of these self-trapped excitons in AgCl [17]. The complete g-tensor of the copper site of the protein azurin was determined by single-crystal ESE spectroscopy at 95 GHz [18]. Different optically excited electronic triplet states of the buckminsterfullerene C_{60} in single crystals were examined at 1.2 K [19].

A CW and pulsed DNP (dynamical nuclear polarization) and EPR spectrometer at a microwave frequency of 140 GHz, equipped with a Fabry-Perot cavity was applied to study a FARCS sample [20, 21]. With this heterodyne spectrometer, frozen solutions of GDP and GTP complexes of the protein p21 *ras* were investigated [22]. A precision field-sweep system, consisting of a deuterium NMR spectrometer and a magnet power supply interfaced to a computer workstation, measured and controlled the magnetic field [23]. The salient feature of this high-frequency spectrometer is a high-power gyrotron [24] which generates the microwave radiation for the DNP experiments. In effect, the gyrotron is a cyclotron-resonance maser. Its CW power is 10 W. In pulse mode, a power of 100 W was generated for microwave pulses of between 1 and 20 ns length.

A high-frequency spectrometer covering the whole frequency range up to 600 GHz utilizes far-infrared lasers as millimeter-wave sources [25]. Angular-orientation-dependent EPR spectra of the stable tyrosyl radical within partially oriented photosystem II were obtained at 245 GHz [26]. From the anisotropy of relaxation times and linewidths the spatial arrangement of the tyrosine, the manganese water-oxidizing complex and the non-heme iron ion has been deduced.

Different microwave source types were compared with another 94 GHz EPR system [27]. Depending on the application, i.e., as to whether moderate or high microwave field strengths are required, a varactor-tuned Gunn oscillator is preferable to a klystron. Therefore, Gunn oscillators are advantageous in free-radicals studies, because these radicals exhibit power saturation at or above 1 mW. For applications requiring high B_1 microwave fields, klystrons can provide higher nominal output power as compared to solid-state oscillators. With a cylindrical TE_{013} cavity a sensitivity of the W-band spectrometer better than 10^9 spins per Gauss has been obtained. X-band and W-band EPR spectra from the primary donor cation, P^{+}_{865}, in both protonated and fully deuterated reaction centers of *Rhodobacter sphaeroides* R-26 directly reflect the improvement of spectral resolution at higher frequencies [27]. Another example for the enhancement of accuracy by high-frequency EPR is a linewidth study of phenyl- and trichloromethyl-PBN (phenyl *tert*-butylnitrone) adducts in benzene [28].

The increasing number of high-frequency-EPR experiments and the high-quality work of some outstanding research groups were arguments for Bruker to develop and offer high-frequency spectrometers commercially designed for a wide range of applications with an exceptional high technical performance. In the following the key elements of the ELEXSYS E600/E680 CW/FT-EPR and ENDOR spectrometer series are described.

2 Frequency Selection: 94 GHz

As mentioned in the introduction, high-frequency EPR can be done at many frequencies. According to the splitting ΔB_0 of two lines with g-factors g_1 and g_2,

$$\Delta B_0 = \frac{h\nu}{\beta}\left(\frac{1}{g_1} - \frac{1}{g_2}\right) \tag{1}$$

the spectral resolution is proportional to the microwave frequency ν (h and β are Planck's constant and the Bohr magneton, respectively). Therefore, one would like to select the highest possible frequency for maximum resolution. Note, however, that the magnetic field required for the resonance condition increases proportionally. In case of Zeeman interaction, the energy at a magnetic field B_0 is

$$h\nu = \beta g B_0 \ . \tag{2}$$

In special cases when large zero-field splittings contribute to the energy it is possible to match the resonance condition at much lower fields using the same high frequency. But most EPR samples give rise to signals in the $g = 2$ region. Therefore, one key factor limiting the spectrometer frequency is the necessary magnetic field. Superconducting magnets provide high magnetic fields with reasonable electric power consumption. Currently, standard superconducting solenoids reach stationary fields up to about 20 Tesla. In case of $g = 2$, this corresponds to an upper spectrometer frequency of about 600 GHz.

However, some constraints will lower this upper limit of 600 GHz. First, for $g < 2$, the maximum field for a given magnet lowers the upper resonance frequency. In addition, since the high-resolution aspect of a high-frequency spectrometer stretches out a spectrum, the sweep range required for spectra acquisition can be rather large. This means that a well-designed EPR spectrometer should offer magnetic fields which are much larger than the field required for the resonance for $g = 2$.

Second, for the majority of the EPR applications, the magnetic field is swept over the spectrum. This kind of operation is completely different from nuclear magnetic resonance (NMR). An NMR magnet is energized once, then set to persistent mode, and NMR spectra are measured without sweeping the field. During installation of an NMR spectrometer it may happen that the magnet quenches. This means that a small portion of the superconducting wire becomes resistive and the high current through the wire heats up the whole magnet and its electromagnetic energy is dissipated in a short time. The magnet must be cooled down again and the energization procedure is started again. For practical EPR spectroscopy the probability of a magnet quench must be much lower than for other applications of superconducting magnets. The solution is to operate an EPR superconducting magnet always far below its maximum achievable field. In other words, the spectrometer frequency must be chosen much smaller than the maximum possible value according to Eq. (2). In this way, the upper frequency limit of a *practical* high-frequency EPR spectrometer is in the range of 300 GHz.

Third, the cost of microwave components increases more than linearly with frequency. The reason for this is that with decreasing wavelength the components must be made smaller and smaller. In addition, the sensitivity of wires and semiconductors against electrical discharge and EMI (electromagnetic interference) increases dramatically with decreasing size. For a routinely operating spectrometer, microwave components must be produced at a reasonable price and they must be serviceable with justifiable efforts.

Fourth, for maximum sensitivity it is recommended to use cylindrical type resonators [7, 29]. The size of the resonators naturally decrease with frequency and the sample preparation becomes more and more cumbersome especially when samples have to be kept and transferred frozen to the already pre-cooled probehead. With these arguments in mind the operating frequency of the E600/E680 series has been selected to W-band (94 GHz). This frequency is sufficiently high enough to get a remarkable increase in resolution and still allows a reasonable sample handling.

The resonance frequency in W-band corresponds to wavelengths in the order of 3 mm. For this reason the term millimeter-wave EPR is commonly used. A typical resonator size is of the order of one wavelength. This implies that the typical sample size is in the same millimeter range. Of course, the ease of sample handling and preparation depends on the type of sample. Sample tubes with dry powder may be prepared in a straightforward way. With special small syringes and pipettes, liquid samples are loaded into the sample tubes. These small capillaries with relatively thick walls help to avoid the breaking of sample tubes while freezing or thawing the sample. Note, however, that small (sub-millimeter) single crystals might just have the proper dimensions for 3 mm EPR spectroscopy.

In RADAR technology, W-band refers to the microwave frequency range from 80 to 110 GHz. The actual reason for 94 GHz as the operating frequency is that microwave absorption of molecular oxygen is at minimum around this frequency. Another aspect of this frequency selection is that critical W-band microwave components must not operate at their respective specification limits. In general, there is no scientific reason to distinguish between EPR spectra taken at, say 105 or 95 GHz. The difference of ten percent in operating frequency shows up as a difference of 10% or less in line splittings. Note that the spectra recorded at 94 GHz reach about ten times the spectral resolution as those recorded at the common X-band (9–10 GHz) frequency.

3 W-Band Microwave Bridge Design

Millimeter-wave components are expensive to make and very sensitive to handling. A microwave bridge, and even more a pulsed microwave bridge contains many components which must be optimized for the needs of EPR. It is possible to construct a millimeter-wave bridge with a concept similar to that of standard EPR microwave bridges. The employment of attenuators, phase shifters, and microwave switches operating at high frequencies sets high expectations for their performance. The high performance requirements face practical production limits. In this case high losses and standing waves lead to compromises in spectrometer stability and EPR sensitivity. An indication of the manufacturing quality of the W-band components can be obtained from the tune picture display of the instrument. A typical tune picture of the W-band cavity with a loaded *Q* of 3000 is shown in Fig. 1. A frequency sweep range of 400 MHz centered at 94.0 GHz was applied. Misalignment of wave guide junctions, poorly fabricated wave guide transitions or a damaged cavity would show up as additional standing wave patterns in the tune picture. The TeraFlex probehead is tunable over a frequency range of more than 10 GHz. In addition, for tuning purposes, the ELEXSYS E600/E680 spectrometers provide an operation bandwidth of 0.8 GHz around 94 GHz.

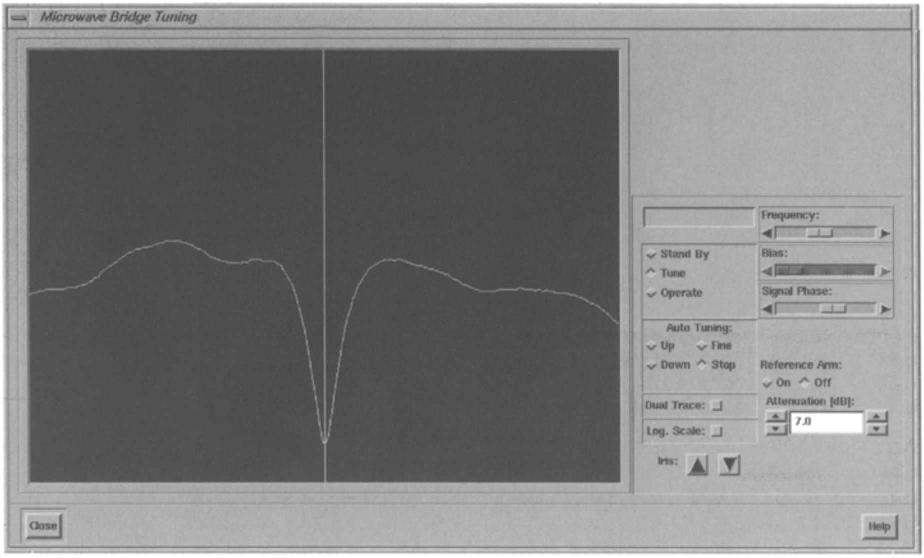

Attenuation [dB]: 7.0

Fig. 1. Tune picture over a 400 MHz sweep range showing the resonance of the TE_{011} cavity at 94.0 GHz. Note, the ordinate is given on a linear scale. (Snapshot taken from the Xepr software.)

Extensive experiments with respect to design concepts have been made at the Bruker high-frequency labs. The achievable signal-to-noise ratios of a homodyne and a heterodyne bridge setup were compared. For bridges operating at 94 GHz, it turned out that the optimum performance with respect to the signal-to-noise ratio is achieved with the heterodyne microwave design. Furthermore, the heterodyne concept offers considerable advantages on other performance aspects like precise determination of the microwave frequency, high dynamic range and linearity of the microwave power, flexibility in pulse timing including phase control as well as component reliability and ease of handling.

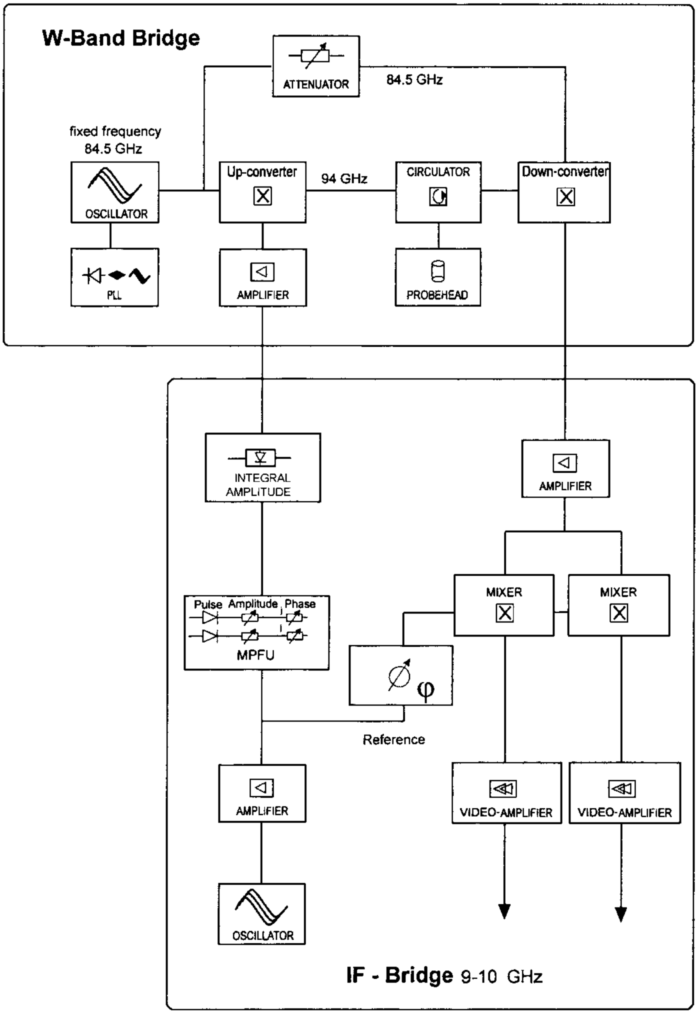

Fig. 2. Schematic block diagram of a heterodyne pulse concept with W-band and IF microwave bridges. Each channel of the multiple-channel microwave pulse former unit (MPFU) features a switching diode, an attenuator and a phase shifter. Following combination of the pulses after the MPFU, all pulse amplitudes are attenuated by the same degree by the integral amplitude attenuator.

The microwave bridge design of the ELEXSYS E600/E680 spectrometer is heterodyne with an IF unit and a W-band bridge. The IF unit can be operated in either CW or pulsed mode at frequencies around 9.5 GHz. The pulse IF unit comprises the microwave attenuator, the pulse-shaping components, phase shifters, broadband detection assemblies as well as the X-band frequency counter. The main components of the W-band bridge are the oscillator, and the highly optimized up- and down-converter. In Fig. 2, the heterodyne microwave bridge design of the pulse W-band bridge is shown. The excitation signal at IF level is up-converted to W-band frequency and transmitted directly to the cavity. The signal from the cavity is directly down-converted to the IF for low-noise signal amplification and detection. The oscillator of the W-band bridge is phase-locked at a frequency of 84.5 GHz. From the known frequency of the 84.5 GHz local oscillator and the counted X-band frequency, the W-band operating frequency is determined, a prerequisite for absolute *g*-factor measurements. In the spectrometer setup the W-band bridge is located close to the probe containing the millimeter-wave cavity to reduce unavoidable losses on the way to and from the cavity. The W-band bridge is constructed for operation in the high fringe fields of the superconducting magnet. Because of the low-noise IF amplifier located in the W-band bridge, the distance between IF-X-band unit and the W-band bridge is irrelevant regarding system stability

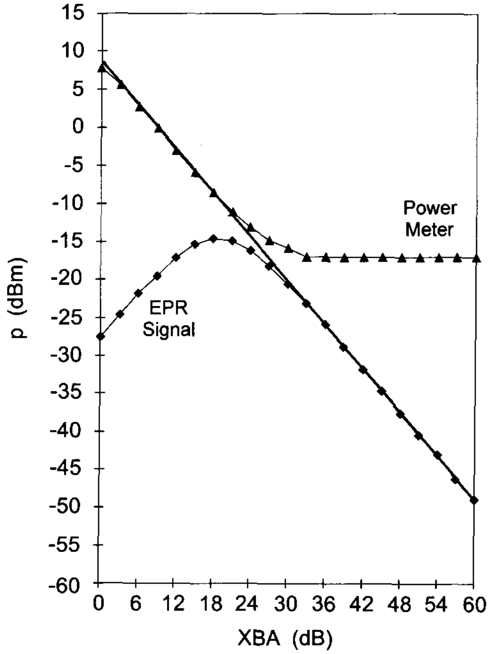

Fig. 3. Microwave power dynamics demonstrated as measured W-band power (top trace, filled triangles) and EPR signal (bottom trace, filled squares) vs. X-band attenuation (XBA). See text for details.

and EPR sensitivity. The IF unit is placed further away from the magnet with no compromises in performance.

As an example for the precision of up- and down-conversion regarding power levels, two power relevant measurements are shown in Fig. 3. The abscissa in both measurements is the IF attenuator setting (XBA) which is in decibel. Two different measurements were performed to cover the full power range of the W-band bridge from 5 mW (at 0 dB) to 60 dB attenuation. In the low-power range up to 30 dB attenuation, W-band EPR signal intensities from manganese ions in calcium oxide were measured. The 1 dB/dB slope in the low-power range shows the quality of the converters and their linearity. At higher-power levels this particular sample shows EPR saturation and the signal amplitude deviates from the straight line. In the high-power range between 0 and 20 dB XBA, a W-band power meter was used. This gives access to the performance of the up-conversion, indicating that almost the full dynamics on the IF side is converted to W-band microwaves. Between 0 and 3 dB, the small deviation from linearity reflects the onset of saturation of the up-converter.

The full microwave power is rarely used for CW-EPR, since many samples saturate even at room temperature at a few milliwatts (typical 2 mW) of W-band power in the millimeter-sized cavity. For instance, in X-band a highly concentrated DPPH sample can partially be saturated with a power of 50 mW, while it only requires 1 mW to attain the same saturation level in the W-band TE_{011} cavity. The high efficiency of the cavity also allows reasonably short microwave $\pi/2$ pulses with 5 mW of power. A microwave field $B_1 \approx 0.9$ G, corresponding to a $\pi/2$ pulse of 100 ns, is obtained at a loaded Q-value of about 3000, i.e., 30 MHz bandwidth. This cavity bandwidth allows still shorter pulses of about 30 ns. With the same amount of power, the corresponding flip angle is reduced. The effect of a flip angle smaller than $\pi/2$ on the sensitivity can be compensated by a corresponding increase in the pulse sequence repetition rate [30] (see below).

4 Hybrid Split-Coil 6 Tesla EPR Magnet

The hybrid magnet design is a flexible solution for the requirement of both, wide field sweeps and adjustments over several Tesla and narrow field sweeps with sub-Gauss resolution and low helium consumption. The magnet consists of a superconducting magnet and a water-cooled room-temperature magnet. The superconducting magnet provides fields from 0 to 6 Tesla (60000 Gauss) and can be set in persistent mode at any field in this range. The homogeneity is specified with <10 ppm over 10 mm diameter spherical volume. Taking into account that W-band samples have dimensions of typically 1 mm, a field homogeneity of about 30 mG is achieved for signals at $g = 2$. The field generated by the superconducting coil can be set with a resolution of 60 mG. The room-temperature magnet produces an offset field from -40 to $+40$ mT (± 400 Gauss) to the persistent field of the superconducting magnet. These field sweeps of up to 80 mT (800 Gauss) with the room-temperature magnet are very useful for EPR studies on free radicals and organic samples around $g = 2$ with the superconducting magnet being persistent at 3.35 T (33500 Gauss).

One important consideration of wide field sweeps with the superconducting magnet is their speed. Using an electromagnet, the EPR spectroscopist usually does not need to consider optimizing the sweep rate. In comparison, the inductance of a superconducting magnet is large. The high field at a reasonable current can only be produced using tens of thousands of turns for winding the superconducting coil. Consequently, the induced voltage caused by magnetic field sweeps can amount to several volts. In case of a quench where the field drops very rapidly, the induced voltage could increase to even a dangerous level. For safety reasons, all superconducting magnets contain limiting diodes which become conductive if the magnet voltage increases over a certain value. On the other hand, these unavoidable diodes limit the sweep speed of a given magnet. The ELEXSYS E600/E680 magnets can be swept using 3 V of induced voltage. At this voltage the sweep rate of the field amounts up to 100 mT per min (1000 Gauss per minute). This sweep rate is fast compared to the rates used for the energization of an NMR magnet.

It is well known that the field behavior of superconducting magnets shows hysteresis effects. For NMR magnets, this is acceptable, since they are charged once to a certain field and stay in persistent mode. For EPR magnets, however, sweeping of the superconducting field is required. For such field sweeps conducted at relatively high rates, the apparent resonance positions of a line acquired during sweeping the field upwards and downwards are shifted with respect to each other by a couple of hundred mT (several thousand Gauss). This effect is due to the additional electrical components inside the magnet.

The type of the field hysteresis depends on how the magnetic field is controlled. There are basically two ways, one is direct current control with high-precision field/current calibration, the other is current control with high-precision field measurement and regulation [23]. The latter has the disadvantage that the magnetic field cannot be measured directly at the sample position. The field detector in a E600/E680 system can only come as close as a few centimeters to the sample, because for reliable field measurement the detector must be positioned outside the sample cryostat. The high magnetic fields at the magnetic center imply that there are high magnetic field gradients in its vicinity. A few centimeters away from the magnetic center the field gradients are of the order of several mT/cm (several tens of Gauss per centimeter). As a consequence the linewidth of a field probe is increased by the field gradient. High-precision field measurements at relatively high speed are therefore difficult for the current regulation of the power supply.

The ELEXSYS W-band spectrometers use therefore high-precision field/current calibration for magnetic field control. With an EPR sample exhibiting narrow lines calibration right at the sample position is performed. Mn^{2+} in CaO, in which the manganese ions occupy purely cubic sites, serves as the calibration sample. The EPR spectrum shows six hyperfine lines of equal intensity with a

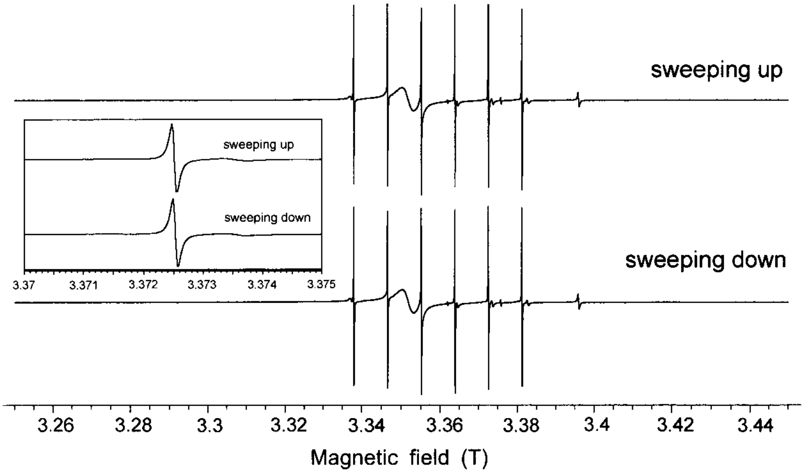

Fig. 4. CW-EPR spectrum of Mn^{2+} in CaO obtained by sweeping the superconducting magnet over 200 mT (2000 G). Inset: expansions of the 200 mT (2000 G) up- and downfield field sweeps after calibration of the superconducting magnet.

linewidth of 70 μT (700 mG) at room temperature. At 90 K, a minimum linewidth of 32 μT (320 mG) has been determined. At room temperature, a larger linewidth of 150 μT (1.5 Gauss) has been reported [31]. The W-band CW-EPR spectrum of such a calibration sample is shown in Fig. 4. Depending on the swept direction of an uncalibrated magnet, the manganese lines appear shifted. The hysteresis can be reduced by taking into account the field/current calibration value and the magnet's inductance by a suitable current pre-emphasis. The result obtained with a carefully calibrated magnet is shown in Fig. 4. In the inset, the expansion of the same data set of the region around the fifth manganese line demonstrates that the hysteresis in this case is smaller than 10 μT (100 mG). If the site of the magnet is chosen properly, the calibration is precise to better than 10^{-5} of the magnetic field. Note that steel reinforcement in walls and floors may lead to field distortions. However, fast field sweeps with high precision are somewhat contradictory. So the dynamic calibration depends on both sweep rates and sweep widths. Obviously, the slower the sweep, the higher the accuracy for determining linewidths and shapes.

The split-coil design of the 6 T EPR magnet has the advantage that the sample cryostat, the probe, and the sample holder are inserted into the magnet perpendicular to the direction of the magnetic field. A similar topology in the electromagnet of lower-frequency systems has proven to be ideal. Sample exchange from the top is done without the need to remove any waveguide connection and without removing the probehead. Even cold samples can be loaded into the pre-cooled probe. This optimizes measuring time very efficiently. Another advantage is that orientation-dependent studies can be performed very easily. Single crystals and/or oriented samples can be rotated perpendicular with respect to the magnetic field by just rotating the sample holder at the top of the magnet.

The ELEXSYS E600/E680 spectrometers can be connected to magnets of other design principles if the magnet bore size fits the probehead dimensions. For applications which require mainly sweeps larger than 800 G, split coil magnets with permanently connected current leads may be more useful with respect to helium consumption.

5 Continuous-Wave EPR Sensitivity

Dependent on a number of spectrometer settings, the EPR spectrum of a sample containing n_s spins shows up with a certain signal-to-noise ratio, *SN*. Below saturation of the EPR transitions, *SN* increases proportional to the microwave field B_1 in the cavity or proportional to the square root of incident power, p. However, this is only valid when oscillator noise is not dominant in the spectrum. This is normally the case for a well tuned, critically coupled cavity.

A reasonable gauge for assessing and comparing spectrometer sensitivities is the minimum number of detectable spins, s_{min}, per 10^{-4} T (1 Gauss) linewidth per square root of seconds measuring time. To this end, the applied microwave power p is normalized to the maximum spectrometer power p_0 at 0 dB attenuation. Generally, the signal-to-noise ratio can always be increased by choosing longer integration constants. The influence of measuring time is taken into account with the square root of the conversion time C_T normalized to one second. If there is more than one EPR line, *SN* must be multiplied with the number of lines, n_L, because the signal would increase by a factor n_L if all spins would contribute to a single line. In general, if the lines have different intensities, n_L must be weighted correspondingly. In case of Mn^{2+} in CaO with equally intense lines, $n_L = 6$. In a similar way the peak-to-peak linewidth ΔB_{pp} must be taken into account. The spectrometer sensitivity, s, is then given as:

$$s = \frac{\sqrt{C_T / s_{\text{min}}}\sqrt{p/p_0}\, n_s}{n_L \Delta B_{pp} SN} . \tag{3}$$

Equation (3) does not hold for very general cases. It is useful to compare CW-EPR spectra taken from different spectrometers with different parameter settings using the same sample. It is, furthermore, assumed that the modulation amplitude is chosen in an optimum way. For sensitivity comparisons, the modulation amplitude is set equal to ΔB_{pp}. The modulation frequency does not play any role unless there is a noise contribution by mechanical or acoustical vibrations which should be avoided. The Bruker W-band TeraFlex probehead can be operated with up to 30 G modulation amplitude at 100 kHz. The sweep time over the spectrum must be chosen slow enough to avoid relaxation or rapid scan effects on the signal amplitude.

For all practical CW-EPR spectroscopy it is important to optimize microwave power. From Eq. (3) it seems that the more power a spectrometer provides, the higher its sensitivity. But, of course, for each sample the maximum power for the measurement depends on its saturation behavior. For comparing different spectrometers with different resonators it is important to ensure that the same B_1 fields are produced in the sample volume. This might quantitatively be very difficult, although B_1 fields can directly be measured with pulsed EPR nutation

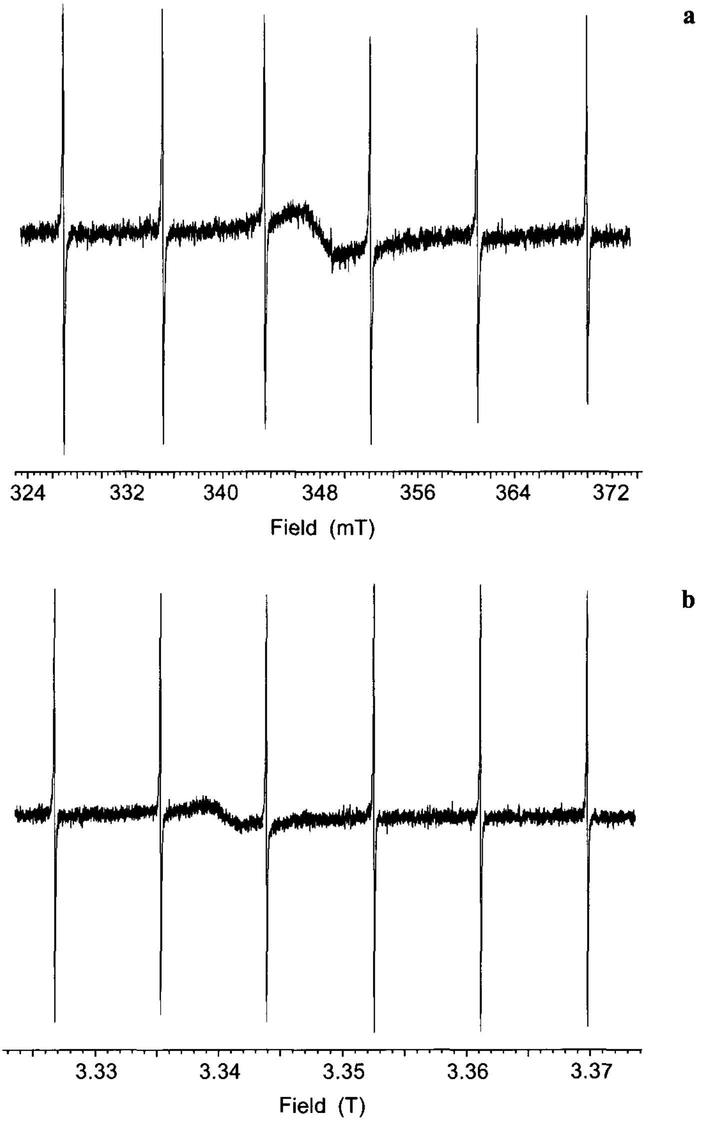

Fig. 5. Comparison of X- and W-band CW-EPR sensitivity. **a** X-band CW-EPR spectrum from a sample of Mn^{2+}:CaO prepared for W-band spectroscopy. **b** W-band CW-EPR spectrum of the identical sample. Note the different position of the broad free-radical line with respect to the narrow six manganese lines. See text for details.

experiments. For the comparison of spectrometer sensitivity at X- and W-band, two spectrometers have been used where the maximum available power p_0 is adjusted so that the B_1 fields in the different cavities are about the same. The microwave power at 0 dB attenuation of a standard X-band spectrometer of the ELEXSYS E500 series is $p_{0X} = 200$ mW, that of the W-band spectrometers is $p_{0W} = 5$ mW.

Two CW-EPR spectra are shown in Fig. 5 for direct comparison of the sensitivities of the X- and W-band spectrometers. A sample of 600 μg of CaO has been measured in both cases. The X-band spectrum in Fig. 5a has been acquired in a standard rectangular TE_{102} cavity. With the spectrometer settings of $C_T = 40$ ms, $p = 3.1$ mW (18 dB), $\Delta B_{pp} = 70$ mT, the signal-to-noise ratio is $SN_X = 54$. The sensitivity of an X-band spectrometer under the above mentioned conditions has been determined to $s_X = 8 \cdot 10^9$ spins/$G\sqrt{Hz}$.

Then the number of Mn^{2+} ions in the CaO sample is obtained (Eq. (3)) as $n_s = 7 \cdot 10^{13}$.

A comparable signal-to-noise ratio, SN_W, with the same sample at W-band can be achieved only by reducing at least one of the spectrometer settings. In Fig. 5b, the corresponding W-band spectrum is shown. It has been acquired with $C_T = 10$ ms, $p = 5$ nW (60 dB), $\Delta B_{pp} = 70$ μT. The signal-to-noise ratio is determined to $SN_W = 85$. With the number of Mn^{2+} ions of $n_s = 7 \cdot 10^{13}$ obtained from the X-band spectrum, Eq. (3) leads to a sensitivity of the W-band spectrometer of $s_W = 2 \cdot 10^7$ spins/$G\sqrt{Hz}$.

Thus, the ELEXSYS E600/E680 W-band spectrometer is about 400 times more sensitive than the X-band spectrometer, for this sample, extrapolated to full available power.

Obviously, this comparison takes into account that both the quality factors, Q_X and Q_W, of the respective cavities indirectly influence the power levels used for the calculation. In general, the higher the Q, the higher the sensitivity if demodulation at phase noise is not a problem. It is also apparent that the numbers for sensitivity given above are absolute numbers of spins. Sensitivity is proportional to filling factor. If sample concentration can be kept constant, a much larger sample volume at X-band more than compensates the higher absolute sensitivity in W-band. However, W-band spectrometers are advantageous in case of precious samples which are available only in small quantities, such as isotopically enriched or specifically labeled compounds as well as biological and/or genetically modified material. High-field spectrometers may also be advantageous for single-crystal studies: It might be impossible to grow crystals as large as required for X-band studies.

5 FT-EPR in W-Band

The multiplex advantage of FT-EPR spectroscopy allows the acquisition of an EPR spectrum in a single-shot experiment. By averaging a large number of transient signals, FT-EPR sensitivity is expected to be higher compared to CW-EPR. In NMR where sampling rates up to 1 MHz and repetition times in the ms range are usually sufficient, the theoretical gain in sensitivity of FT-NMR compared to CW methods was realized 30 years ago. However, the large coupling constants and excitation bandwidths involved in EPR require sampling rates of several hundred MHz. Furthermore, spin-lattice relaxation times in EPR can easily be in the sub-ms range and require correspondingly fast averaging capabilities for optimum signal-to-noise. In the past, sensitivity of pulsed EPR was limited due to the lack of transient recorders with high sampling rates and high averaging speed. This bottleneck was overcome only recently with the introduction of the Bruker SpecJet, a high-speed transient-signal averager for FT-EPR. The SpecJet is able to accumulate up to one million transients per second at a data-sampling rate of up to 250 MHz. It allows averaging in the T_1 (spin-lattice relaxation time) limit for a wide range of samples. The enormous gain in sensitivity has been demonstrated with various samples in X-band [32].

X-band FT-EPR is typically characterized by short (10 ns), high-power (1 kW) microwave pulses, resonators with a Q of 100, a dead-time of about 60 to 80 ns and a duty cycle limit of 1% due to the high-power amplifier. All these key figures are drastically different at 94 GHz. Only a few mW of microwave power is necessary to achieve a $\pi/2$ pulse length of 100 ns at a resonator bandwidth which is similar to X-band. An obvious advantage in W-band is the low dead-time. It has been shown [7, 33] that electron spin nutation signals can be detected even on top of the pulse.

The bandwidth of the W-band TeraFlex resonator is typically in the range of 100 to 30 MHz. Matching the bandwidths of pulse excitation and resonator would allow pulse lengths of 10 to 30 ns corresponding to effective flip angles $\beta \approx$ 10–30°. The loss in sensitivity due to the reduced signal amplitude can be compensated by optimizing the pulse sequence repetition time T according to [30]:

$$\cos\beta_{\mathrm{opt}} = \exp(-T/T_1) \ . \tag{4}$$

where β_{opt} is the optimal flip angle.

For example, if a 16 ns pulse with $\beta = 15°$ is applied, the optimum pulse sequence repetition time is $0.035T_1$. Considering that the SpecJet has a minimum re-trigger time of 1 μs this allows averaging signals with $T_1 \geq 28$ μs under optimum conditions. As there is no duty cycle limit due to a microwave power amplifier there is no additional limitation.

As an example both the CW-EPR and the FT-EPR spectrum of the endohedral fullerene N@C_{60} (A. Weidinger, pers. commun.), [34] in C_{60} are shown in Fig. 6. The three narrow lines are caused by the hyperfine coupling to the nitrogen, ^{14}N. The CW-EPR spectrum has been acquired during a field sweep lasting 20 seconds with the microwave power set to 59 dB (0 dB = 5 mW) just slightly saturating the EPR signal. The modulation amplitude was set equal to the linewidth of 200 mG. For the FT-EPR spectrum 180000 free-induction decays (FIDs) have been accumulated in 20 seconds including a 4-step phase cycle for baseline correction and image cancellation. The FT-EPR spectrum was obtained by zero filling the FID from 1 to 4 k points, Fourier transfor-

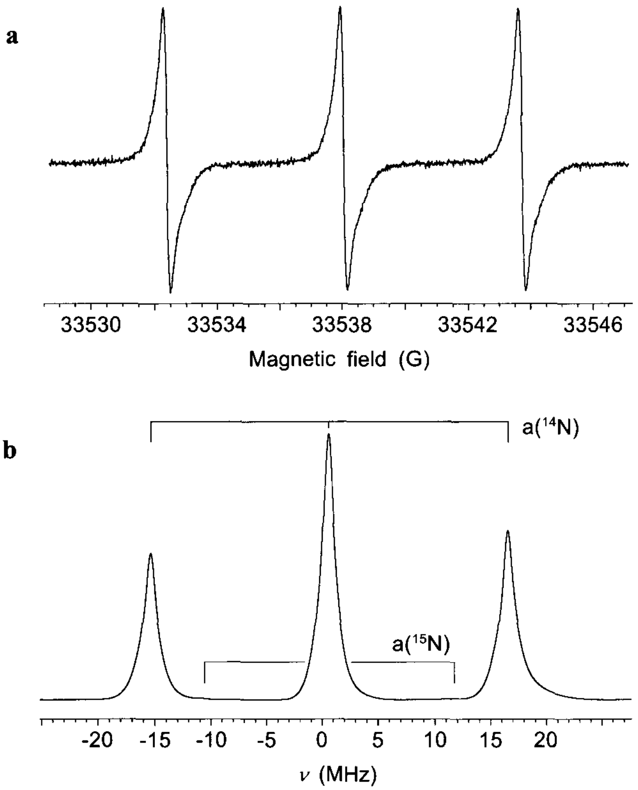

Fig. 6. Comparison of the W-band FT-EPR and CW-EPR spectra of a powder sample of the endohedral fullerene N@C_{60} in C_{60} measured at room temperature. In both experiments, the total acquisition time was set equal to 20 s. **a** W-band CW-EPR spectrum of N@C_{60}. Modulation amplitude, 0.2 G (100 kHz); number of field positions, 1024; microwave power, 59 dB. **b** W-band FT-EPR spectrum of N@C_{60}. Pulse length, 16 ns; shot repetition time, 102 ms; dead-time, 30 ns; 1024 time domain data points; sampling rate, 250 MHz; field value, 33538.2 G; number of accumulations, 180000. Processing parameters: zero filling to 4 k points; Fourier transformation with phase correction. Note: The FID was not filtered by a window function; the FT spectrum was not corrected for the cavity bandwidth of about 38 MHz.

mation and linear phase correction. Note a window function for *SN* improvement was not applied. In both those experiments the resonator was critically coupled to a *Q* of 2500 corresponding to 38 MHz bandwidth. The FID was excited by a pulse of 16 ns which would allow a spectral coverage of about 60 MHz, however, the cavity bandwidth sets the limit to 38 MHz. The amplitude ratios of the three lines directly reflect this cavity bandwidth. To measure even broader spectra, like spin labels in solution, the resonator bandwidth could be further increased by overcoupling. It is noted in passing that although the intensities of the FT-EPR lines do not reflect the expected amplitude ratio (1 : 1 : 1), deconvolution with the known bandwidth will give the correct amplitude ratio. More important, due to the fact that high-frequency

FT-EPR is feasible, the main prerequisite for high-field 2D correlation studies, like ELDOR, COSY and SECSY is fulfilled. The prime aim of these studies is to look for cross-peaks giving access to information about molecular dynamics and spin-spin couplings.

To optimize *SN* of the FT-EPR spectrum (Eq. (4)), the pulse repetition time was set to 102 μs. With $\beta \approx 15°$ and $T_1 \approx 2$ μs, the measuring condition was close to optimum. Evaluating the signal-to-noise ratio of the CW and the FT spectrum, we obtain $SN_{\mathrm{CW}} = 55$ and $SN_{\mathrm{FT}} = 1400$. The gain in FT *SN* compared to CW is considerably higher than in X-band for a similar spectrum. This is due to the fact that the resonator bandwidth and coupling remains constant when changing from CW to FT operation. In X-band, on the other hand, the Q has to be lowered drastically when switching to FT in order to achieve the required bandwidth and dead-time. The remarkable gain in sensitivity for the FT spectrum is also reflected in the detection of the ^{15}N lines as indicated in Fig. 6.

It must be pointed out that a quantitative comparison requires some more considerations. In many cases the conventional FT technique cannot be applied in EPR because of an insufficient excitation and detection bandwidth. In such cases, electron-spin echo (ESE) detection combined with a magnetic field sweep is performed. The multiplex advantage is lost. However, the ability to average the echo in the T_1 limit is now even more important. On the other hand, improving the signal-to-noise ratio in CW-EPR might not be easy as well. Effects of microwave power saturation as well as the influences of modulation amplitude and frequency on the EPR lineshape must be taken into account. In addition, in case the EPR spectrum is the superposition of sub-spectra from different species, CW-EPR might not be capable of separating them. However, ESE detection may lead to a separation, due to differences in the spin-spin and/or spin-lattice relaxation times of the contributing species.

6 W-Band Pulsed ENDOR Experiments

If an electron spin ($S = 1/2$) exhibits (different) hyperfine couplings (hfc's) to k different, N_i equivalent nuclear spins I_k, the EPR spectrum would consist of $\Pi^k(2N_iI_k + 1)$ different resonance lines. In contrast, the corresponding ENDOR spectrum would consist of only $2k$ lines. Obviously, the ENDOR spectrum reduces complexity. Moreover, the ENDOR spectrum of a broad featureless EPR line may reveal the underlying set of hfc's. The ENDOR spectrum also includes information about the nuclear entities itself via their respective nuclear Larmor precession frequencies, $\nu_{\mathrm{N}}(I)$.

Since ν_{N} scales with the magnetic field in the same way as the EPR frequency does, high-field ENDOR would be advantageous due to the following.

1. At W-band the Larmor frequencies are spread over almost 150 MHz as compared to 15 MHz at X-band. Overlapping lines at X-band originating from different nuclei become separated at W-band.

2. Orientation-selective ENDOR experiments of powder and/or disordered samples [35] become both more selective the higher the field and feasible for much more samples. Due to the increased resolution in the EPR spectrum, the dependence of the ENDOR spectrum on the EPR field position, i.e., the projection of the principal A-tensor axes into the g- (or zero-field splitting) tensor axis system, can be obtained.

A new W-band ENDOR resonator has been developed. In order to cover the nuclear Larmor frequency range at W-band from a few MHz (e.g., ^{57}Fe, ^{89}Y) to nearly 150 MHz for the protons, a probehead matched to the ^{1}H frequency has been designed. The probe has the same microwave mode as the standard resonator, TE_{011}. For other nuclei the probe can be switched to a broad-band setup. Pulsed electron nuclear double resonance experiments can be performed at 94

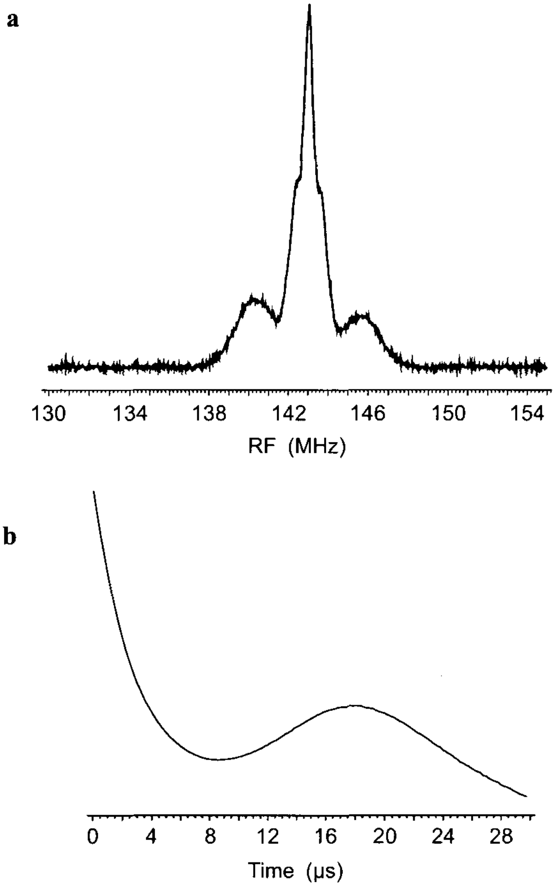

Fig. 7. **a** W-band Davies ^{1}H-pulsed ENDOR spectrum of a BDPA powder sample in polystyrene. Experimental parameters: RF pulse length, 8 μs; microwave preparation pulse, 560 ns; integration of the echo intensity. **b** Radio frequency transient nutation experiment at W-band on a coal sample. Davies pulse sequence with FID detection. 150 points with 200 ns/point.

GHz microwave frequency without loss in EPR sensitivity, i.e., the EPR Q-value stays constant. Due to the design of the RF coil, the volume ratios between the sample volume and the microwave cavity on one side and between the sample and the RF coil are approximately the same. Thus, only moderate RF power amplification is required to achieve RF π-pulse lengths of well below 10 μs (RF power amplifier, p_{out} of max. 200 W) (see below).

Some examples of W-band pulsed ENDOR experiments are given in Figs. 7 and 8. In Fig. 7a, the Davies ^{1}H-pulsed ENDOR spectrum of a BDPA powder sample in polystyrene is depicted. In this experiment, the RF pulse length was 8 ms. The integral of the echo was recorded as a function of the RF frequency. In Fig. 7b, an RF transient nutation experiments is shown to assess the B_2 field strength incident on the sample. The time trace was acquired at the free-proton Larmor frequency of a coal sample. With the 200 W RF amplifier, the resulting π-pulse length is approximately 8 μs. This corresponds to a B_2 field strength of about 15 G.

In Fig. 8, a Mims pulsed ENDOR spectrum is displayed between 10 and 40 MHz. The sample was N@C$_{60}$. In this case, the RF pulse length was set to 28 μs. Since the electron spin is $S = 3/2$, four ENDOR lines are expected for the nitrogen nucleus, two for $m_s = 1/2$ and two for $m_s = 3/2$. In addition, the hfc of ^{14}N ($I = 1$) is larger than the nuclear Larmor frequency, thus, the lines from the $m_s = 3/2$ manifold are separated by $2\nu_N(^{14}\mathrm{N})$. The high-frequency line at 35.9 MHz is assigned to ^{13}C from the C$_{60}$ cage surrounding the nitrogen. The different amplitudes of the nitrogen lines approximately reflect the difference in nuclear enhancement expected for the two different electron spin manifolds.

Comparison of the pulsed ENDOR experiments with matched and broad-band setups reveals that in case of the latter the applied RF pulse length is larger by a factor of 3–4. Note, however, that the same RF power amplifier (200 W) has been used. Thus, even in case of the broad-band setup, acceptable short RF pulse lengths are achieved with only moderate power amplification of the RF.

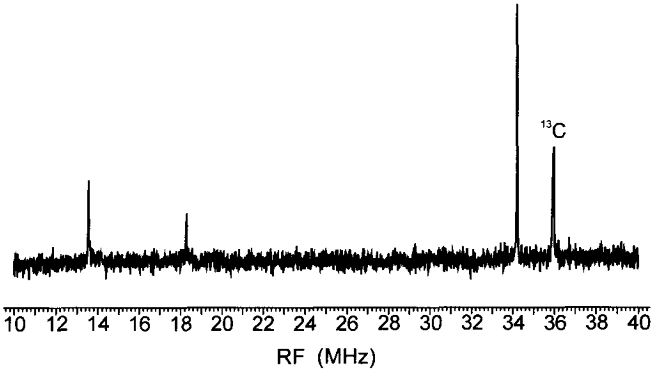

Fig. 8. W-band Mims pulsed ENDOR spectrum of a powder sample of N@C$_{60}$. Shown is the RF range between 10 and 40 MHz. RF pulse length, 28 μs. Microwave pulse length, 180 ns. The magnetic field was set to the maximum of the low-field EPR line.

7 Conclusions

The Bruker ELEXSYS E600/E680 series CW/FT-EPR and ENDOR W-band spectrometers are a powerful as well as a flexible tool for analytical applications in the fields of physics, chemistry, biology, and geology.

With the choice of 94 GHz for high-frequency EPR, Bruker has selected a microwave frequency for an optimum compromise between resolution, sensitivity, sample size, handling, technical reliability, and practical daily work. The heterodyne microwave bridge design guarantees maximum sensitivity and converts the flexibility of X-band spectrometers to W-band instrumentation. The combined design of the split-coil superconducting magnet and the sample cryostat – housing the TeraFlex probe – allows an easy sample exchange at any temperature down to 4.2 K. However, the E600/E680 systems are not tied to this magnet type. Superconducting magnets of different design and from different manufacturers can be operated with the ELEXSYS E600/E680 spectrometers, if they comply with the probehead design. The high-Q W-band resonator delivers maximum sensitivity. It is tunable over more than a 10 GHz range and can be used with field modulation amplitudes up to 3 mT (30 G). The spectrometer control software provides assistance for safe operation of the magnet and is fully integrated in the Xepr frame, the comprehensive and most sophisticated software package which has ever been written for EPR spectrometers. The PatternJet pulse programmer and the SpecJet transient-signal averager set a new benchmark in time-domain EPR, making also true FT-EPR in W-band a reality. The application range of the ELEXSYS instruments is considerably extended with the new pulsed ENDOR probehead.

With its high sensitivity, high resolution and professional design, these W-band high-field/high-frequency spectrometers have set new perspectives and standards to EPR spectroscopy.

Acknowledgements

We would like to thank Prof. K. Holczer (UCLA, Los Angeles, USA) for his contribution in the initial stage of the W-band project. Further, the authors acknowledge Prof. A. Weidinger and Dr. B. Pietzak (Hahn-Meitner-Institute, Berlin, Germany) for providing the N@C_{60} sample, and Dr. R. T. Weber (BRUKER Inc., Billerica, USA) for preparing the BDPA sample. Finally, we note that design, development and production of the W-band system took place at the EPR division of the BRUKER Analytik GmbH at Rheinstetten, Germany.

References

1. Hoff A.J. (ed.): Advanced EPR: Application in Biology and Biochemistry. Amsterdam: Elsevier 1989.
2. van Keand L., Bowman M.K. (eds.): Modern Pulsed and Continuous Wave Electron Spin Resonance. New York: Wiley & Sons 1990.

3. Grinberg O.Ya., Dubinskii A.A., Shuvalov V.F., Oransky L.G., Kurochkin V.I., Lebedev Ya.S.: Dokl. Acad. Nauk USSR **230**, 884 (1976)
4. Poluektov O.G., Grinberg O.Ya., Dubinskii A.A., Luk'yanenko L.V., Sidorov O.Yu., Lebedev Ya.S.: Russ. J. Phys. Chem. **62**, 1067 (1988)
5. Bresgunov A.Yu., Dubinskii A.A., Poluektov O.G., Lebedev Ya.S.: Mol. Phys. **72**, 1132 (1992)
6. Smirnov A.I., Poluektov O.G., Lebedev Ya.S.: J. Magn. Reson. **97**, 1 (1992)
7. Bresgunov A.Yu., Dubinskii A.A., Krimov V.N., Petrov Yu.G., Poluektov O.G., Lebedev Ya.S., Appl. Magn. Reson. **2**, 715 (1991)
8. Haindl E., Möbius K., Oloff B.: Z. Naturforsch. A **40**, 169 (1985)
9. Burghaus O., Heindl E., Plato M., Möbius K.: J. Phys. E Sci. Instrum. **18**, 294 (1985)
10. Burghaus O., Toth-Kischkat A., Klette R., Möbius K.: J. Magn. Reson. **80**, 383 (1988)
11. Klette R., Törring J.T., Plato M., Möbius K., Bönigk B., Lubitz W.: J. Phys. Chem. **97**, 2015 (1993)
12. Prisner T.F., van der Est A., Bittl R., Lubitz W., Stehlik D., Möbius K.: Chem. Phys. **194**, 361 (1995)
13. Lynch W.B., Earle K.A., Freed J.H.: Rev. Sci. Instrum. **59**, 1345 (1988)
14. Earle K.A., Budil D.E., Freed J.H.: J. Phys. Chem. **97**, 13289 (1993)
15. Weber R.T., Disselhorst J.A.J.M., Prevo L.J., Schmidt J., Wenckebach W.T.: J. Magn. Reson. **81**, 129 (1989)
16. Disselhorst J.A.J.M., van der Meer H., Poluektov O.G., Schmidt J.: J. Magn. Reson. A **115**, 183 (1995)
17. Poluektov O.G., Donckers M.C.J.M., Baranov P.G., Schmidt J.: Phys. Rev. B **47**, 10226 (1993)
18. Coremans J.W.A., Poluektov O.G., Groenen E.J.J., Canters G.W., Nar H., Messerschmidt A.: J. Am. Chem. Soc. **116**, 3097 (1994)
19. Groenen E.J.J., Poluektov O.G., Matsushita M., Schmidt J., van der Waals J.H., Meijer G.: Chem. Phys. Lett. **197**, 314 (1992)
20. Un S., Prisner T.F., Weber R.T., Seaman S.A., Fishbein K.W., McDermott A.E., Singel D.J., Griffin R.G.: Chem. Phys. Lett. **189**, 54 (1992)
21. Prisner T.F., Un S., Griffin R.G.: Isr. J. Chem. **32**, 357 (1992)
22. Bellew B.F., Halkides C.J., Gerfen G.J., Griffin R.G., Singel D.J.: Biochemistry **35** 12180 (1990)
23. Un S., Bryant J., Griffin R.G.: J. Magn. Reson. A **101**, 92 (1993)
24. Beccera L.R., Gerfen G.J., Bellew B.F., Bryant J.A., Hall D.A., Inati S.J., Weber R.T., Un S., Prisner T.F., McDermott A.E., Fishbein K.W., Kreisch K.E., Temkin R.J., Singel D.J., Griffin R.G.: J. Magn. Reson. A **117**, 28 (1995)
25. Muller F., Hopkins M.A., Coron N., Grynberg M., Brunel L.C., Martinez G.: Rev. Sci. Instrum. **60**, 3681 (1989)
26. Un S., Brunel L.C., Brill T.M., Zimmermann J.L., Rutherford A.W.: Proc. Natl. Acad. Sci. USA **91**, 5262 (1994)
27. Wang W., Belford R.L., Clarkson R.B., Davis P.H., Forrer J., Nilges M.J., Timken M.D., Walczak T., Thurnauer M.C., Norris J.R., Morris A.L., Zhang Y.: Appl. Magn. Reson. **6**, 195 (1994)
28. Smirnova T.I., Smirnov A.I., Clarkson R.B., Belford R.L., Kotake Y., Janzen E.G.: J. Phys. Chem. B **101**, 3877 (1997)
29. Poluektov O.G., Schmidt J.: Bruker Report **143**, 34 (1996)
30. Ernst R.R., Bodenhausen G., Wokaun A.: Principles of Nuclear Magnetic Resonance in One and Two Dimensions. Oxford: Oxford Science Publications 1987.
31. Goldberg I.B. in: Electron Spin Resonance, vol. 6, p. 1. Oxford: Alden Press 1981.
32. Höfer P. in: Magnetic Resonance and Related Phenomena (Ziessow D., Lubibz W., Lendzian F., eds.), p. 93, Joint 29th Ampere - 13th ISMAR International Conference, Berlin August 2–7, 1998. Technische Universität Berlin: Berlin 1998.
33. Höfer P., Maresch G.G., Schmalbein D., Holczer K.: Bruker Report **142**, 15 (1996)
34. Murphy T.A., Pawlik T., Weidinger A., Höhne M., Alcala R., Spaeth J.-M.: Phys. Rev. Lett. **77**, 1075 (1996)
35. Rist G., Hyde J.S.: J. Chem. Phys. **49**, 2449 (1968)

Authors' address: Dr. Dieter Schmalbein, BRUKER Analytik GmbH, Silberstreifen, 76287 Rheinstetten, Germany